Photonic realization of $\mathcal{PT}$-symmetric quantum field theories

Stefano Longhi and Giuseppe Della Valle
Dipartimento di Fisica, Politecnico di Milano and Istituto di Fotonica e Nanotecnologie del Consiglio Nazionale delle Ricerche, Piazza L. da Vinci 32, I-20133 Milan, Italy
(Received 5 December 2011; published 31 January 2012)

A photonic realization of the quantum field theoretical Lee model, describing the strong coupling of two neutral fermions and a neutral scalar boson field, is proposed in the ghost regime, where the Lee Hamiltonian is non-Hermitian but $\mathcal{PT}$ symmetric. Our optical system, which is based on light transport in an engineered semi-infinite waveguide lattice, could provide an accessible laboratory system to simulate $\mathcal{PT}$-symmetric quantum field theories and to visualize the appearance and role of ghost states in the dynamics.

DOI: 10.1103/PhysRevA.85.012112 PACS number(s): 11.30.Er, 03.65.Ge, 11.10.Gh, 42.79.Gn

I. INTRODUCTION

An unpleasant feature arising in nonperturbative renormalization procedures of relativistic quantum field theories (QFTs) is the "ghost problem," (i.e., the appearance of negative norm states and nonunitary of the S-matrix for strong coupling). Such predictions are generally viewed as a fundamental deficiency for an acceptable QFT [1–3]. This happens, for example, in the Lee model [4], which was introduced in 1954 by Lee as a simple toy model of three interacting fields (two neutral fermion fields and a neutral scalar boson field) in which renormalization can be exactly performed. Källen and Pauli showed that, when the renormalized coupling constant is larger than a critical value, the Hamiltonian of the Lee model becomes non-Hermitian and a ghost state appears [2,5]. Numerous attempts were suggested to make sense of ghost states, for example, by introduction of an indefinite metric in the Hilbert space; however, at the price of giving up microscopic causality and the unitarity of the S-matrix (see, for instance, Ref. [2] and references therein). This was regarded as unacceptable and the Lee model in the ghost regime has been then generally viewed as an unsatisfactory QFT [3]. However, since the advent of $\mathcal{PT}$ quantum mechanics [6–8], there has been a renewed interest in $\mathcal{PT}$-symmetric extensions of QFTs [7,9,10], including the Lee model in the ghost regime [10]. In Ref. [10], Carl Bender and collaborators noticed that, in the ghost regime, the Lee Hamiltonian is not Hermitian, however it does possess $\mathcal{PT}$ symmetry (i.e., it is invariant under combined space reflection and time reversal), and a unitary quantum theory can be constructed by introduction of an appropriate time-independent operator (the $\mathcal{C}$ operator) and a new inner product, in terms of which the ghost state has a positive norm and the Lee model is an acceptable unitary quantum field theory for all values of coupling.

Recently, a great interest has been devoted to the realization of physical systems described by $\mathcal{PT}$-symmetric Hamiltonians [11–20], including optical [12,13,15–19] and electronic [20] systems. In particular, since the pioneering work by Makris, El Ganay, and collaborators [12], it has been recognized that light propagation in engineered photonic structures with balanced optical gain and absorption can provide an experimentally accessible test bed to realize $\mathcal{PT}$-symmetric quantum mechanical theories, with important applications to the realization of nonreciprocal optical devices [19]. Most of such previous studies in the optical context have been mainly focused to the realization of nonrelativistic [12–15] or relativistic [16,18] $\mathcal{PT}$-symmetric quantum mechanical wave equations; however, so far little attention has been devoted to simulate in optics $\mathcal{PT}$-symmetric extensions of QFTs, which is the aim of this work. In particular, here we propose an optical system, based on light propagation in an engineered semi-infinite waveguide lattice, which could provide a test bed to simulate in the laboratory the Lee model in the ghost regime.

The paper is organized as follows: In Sec. II, we briefly review the QFT Lee model in the ghost regime, corresponding to a complex-valued bare coupling constant, and present analytical results for a specific spectral coupling function. The photonic realization of the non-Hermitian model is then presented in Sec. III. Finally, in Sec. IV the main conclusions are outlined.

II. LEE MODEL AND GHOST STATES

A. The model

In this section, for the sake of completeness we will briefly review the QFT Lee model [2–4], focusing our attention on the ghost regime where the Hamiltonian is not Hermitian but $\mathcal{PT}$ symmetric [10]. Such an analysis will be then specialized in Sec. II B by assuming an exactly solvable spectral coupling function and dispersion relation, suggesting a photonic realization of the model in Sec. III.

The Lee model is a rather simple QFT model describing three interacting fields: two fermion fields, describing the V and N particles, and a boson field, describing the θ particles. The V particle can emit a θ particle, transforming into the N particle; however it cannot absorb a θ particle. On the other hand, the N particle can absorb a θ particle, transforming into the V particle, but cannot emit a θ particle. Here we consider a one-dimensional system, so that the momentum of particles is a scalar variable. The Hamiltonian describing the field system (with $\hbar = c = 1$) reads $\hat{H} = \hat{H}_0 + \hat{H}_I$, where [2–4]

$$\hat{H}_0 = m_{V_0} \int dp \hat{V}^\dagger(p)\hat{V}(p) + m_{N_0} \int dp \hat{N}^\dagger(p)\hat{N}(p) + \int dk \Omega(k) \hat{a}_\theta^\dagger(k)\hat{a}_\theta(k) \quad (1)$$

is the noninteracting Hamiltonian, and

$$\hat{H}_I = g \int dk f(k) \int dp [\hat{V}^\dagger(p)\hat{N}(p-k)\hat{a}_\theta(k) + \hat{N}^\dagger(p-k)\hat{a}_\theta^\dagger(k)\hat{V}(p)] \quad (2)$$

describes the interaction of the three fields. In the previous equations, $\hat{N}^\dagger(p)$ [$\hat{V}^\dagger(p)$] and $\hat{N}(p)$ [$\hat{V}(p)$] are the creation and annihilation operators of the fermion N [V] with momentum p, $\hat{a}_\theta^\dagger(p)$, and $\hat{a}_\theta(p)$ are the creation and annihilation operators of the bosons θ, m_{V_0}, and m_{N_0} are the bare masses of the V particle and N particle, respectively, $\Omega(k)$ is the energy of a θ quantum of momentum k, g is the bare coupling constant, and $f(k)$ is the (real-valued) normalized spectral coupling function. The energy $\Omega(k)$ is usually taken to be $\Omega(k) = \sqrt{\mu^2 + k^2}$, where μ is the mass of the boson, and a cutoff function is introduced in the shape of $f(k)$ to avoid divergences [2,3]. However, here we will not specify the form of the dispersion relation $\Omega(k)$, as well as the shape of the spectral function $f(k)$. It is well known that, in the Lee model, the physical and bare one-N-particle and one-θ-particle states coincide; that is, $\hat{N}^\dagger(p)|0\rangle$ and $\hat{a}^\dagger(k)|0\rangle$ are eigenfunctions of $\hat{H}$ with eigenvalues m_{N_0} and $\Omega(k)$, respectively. This is not the case for the physical and bare states of the V particle. The "physical" state $|m_V, p\rangle$ of the V particle, corresponding to the "bare" state $|m_{V_0}, p\rangle = \hat{V}^\dagger(p)|0\rangle$ in the noninteracting ($g \to 0$) limit, is found as a solution of the eigenvalue equation $\hat{H}|m_V, p\rangle = m_V|m_V, p\rangle$ corresponding to a bound state. The eigenvalue m_V is the renormalized mass of the physical V particle. The state $|m_V, p\rangle$ can be represented by the following superposition of the V and N-θ bare scattering states (see, for instance, Ref. [2]):

$$|m_V, p\rangle = \sqrt{Z}\left\{\hat{V}^\dagger(p)|0\rangle + \int dk\,\Phi(k)\hat{N}^\dagger(p-k)\hat{a}_\theta^\dagger(k)|0\rangle\right\}, \tag{3}$$

where $Z = Z(m_V, p)$ is a normalization constant. The renormalized mass m_V is then found as a solution to the nonlinear algebraic equation

$$m_V - m_{V_0} = g^2\Delta(m_V), \tag{4}$$

where we have set

$$\Delta(m_V) = \mathrm{P}\int dk \frac{f^2(k)}{m_V - \omega(k)} \tag{5}$$

and

$$\omega(k) = \Omega(k) + m_{N_0}. \tag{6}$$

Note that, after introduction of the density of states $\rho(\omega) = (\partial k/\partial\omega)$ and the spectral function $G(\omega) = \rho(\omega)f^2(\omega)$, one can write

$$\Delta(m_V) = \mathrm{P}\int d\omega \frac{G(\omega)}{m_V - \omega}. \tag{7}$$

A stable V particle is found provided that a solution m_V to Eq. (4) does exist outside the continuum of N-θ scattering states [i.e., for which $m_V \neq \omega(k)$ for any allowed value of k].

Let us first assume that the bare coupling constant g is real valued (i.e., $\hat{H}$ is Hermitian). Then, the renormalized coupling constant g_r is introduced as [2,3,10] $g_r^2 = Zg^2$, from which one obtains (see, for instance, Ref. [2])

$$g^2 = \frac{g_r^2}{1 - g_r^2 L}, \tag{8}$$

where we have set

$$L = \int d\omega \frac{G(\omega)}{(m_V - \omega)^2} = -\frac{d\Delta}{dm_V}. \tag{9}$$

The value g_r of the renormalized coupling constant is in principle taken from experimental data [2,3]; the value of g is correspondingly retrieved from Eq. (8). For a strong renormalized coupling g_r (i.e., larger than $1/\sqrt{L}$), from Eq. (8) one would obtain an imaginary bare coupling constant, $g = ig_0$ (with g_0 a real number); that is, the Hamiltonian of the Lee model becomes non-Hermitian. This would imply that probabilities are neither conserved nor are they necessarily positive definite, which is generally viewed as an unacceptable result. In addition, a new state with negative norm, which is called a "ghost," appears. Such predictions have been seen as a fault of the Lee theory, which has been thus regarded as nonphysical in the $g_r > 1/\sqrt{L}$ regime (the ghost regime) [3]. However, in Ref. [10], Carl Bender and collaborators showed that, in the framework of $\mathcal{PT}$ quantum theories, the Lee model can be an acceptable unitary quantum field theory for all values of coupling g_r. In the following, we will focus our attention on the ghost regime of the Lee model, assuming an imaginary bare coupling $g = ig_0$. In this case, $\hat{H}$ is not Hermitian (i.e., $\hat{H} \neq \hat{H}^\dagger$); however, $\hat{H}$ is $\mathcal{PT}$ invariant and one has $\hat{H}^\dagger = \hat{H}^*$ (where * stands for complex conjugation), rather than $\hat{H}^\dagger = \hat{H}$. Therefore, for a couple of eigenstates $|\psi_1\rangle \equiv |m_{V1}, p_1\rangle$ and $|\psi_2\rangle \equiv |m_{V2}, p_2\rangle$ of $\hat{H}$ the biorthogonal relations $\langle\psi_1^*|\psi_2\rangle = \delta_{m_{V1},m_{V2}}\delta(p_1 - p_2)$ should be satisfied. From Eq. (3), it readily follows that

$$\langle\psi_1^*|\psi_2\rangle = Z(m_{V1}, p_1)\big(1 - Lg_0^2\big)\delta_{m_{V1},m_{V2}}\delta(p_1 - p_2), \tag{10}$$

where L is defined by Eq. (9). Hence the normalization constant Z should be taken equal to

$$Z = \frac{1}{1 - g_0^2 L}. \tag{11}$$

Therefore, in the non-Hermitian case the sign of Z is not defined; that is, it can be positive (this is the case of the physical V state and the physical N-θ scattering states), but also *negative*, which is the case of the so-called ghost states. For the usual shape of the spectral coupling $f(k)$ and dispersion relation $\Omega(k)$ of the bosonic field, as g_r crosses the limiting value $1/\sqrt{L}$ and $\hat{H}$ becomes non-Hermitian, in addition to the physical V state, corresponding to a positive value of Z, a ghost appears, with opposite sign of Z [2,3,10]. The appearance of this new state can be visualized in the time domain as an oscillatory behavior of the amplitude probability of the bare V state. In fact, let us look for a solution to the time-dependent Schrödinger equation $i\,\partial_t|\psi(t)\rangle = \hat{H}|\psi(t)\rangle$ in the form

$$|\psi(t) = c_0(t)\hat{V}^\dagger|0\rangle + \int dk\,\Phi(k,t)\hat{N}^\dagger(p-k)\hat{a}_\theta^\dagger(k)|0\rangle. \tag{12}$$

The evolution of the amplitude probabilities $c_0(t)$ and $\Phi(k,t)$ of bare V and N-θ scattering states then reads

$$i\frac{dc_0(t)}{dt} = m_{V_0}c_0(t) + g\int dk f(k)\Phi(k,t), \tag{13}$$

$$i\frac{d\Phi(k,t)}{dt} = \omega(k)\Phi(k,t) + gf(k)c_0(t), \tag{14}$$

with $g = ig_0$ in the ghost regime. Note that $c_0(t)$ represents the amplitude probability of the bare V-particle state. Let us assume that, at $t = 0$, the system is in the bare V-particle state [i.e., $c_0(0) = 1$, $\Phi(k,0) = 0$], and that the interaction is switched on at $t = 0$. The amplitude probability $c_0(t)$ can be written in a closed form as a contour integral of the resolvent in the complex plane. If $\hat{H}$ has two bound states, the physical V state and the ghost state with masses m_{V_1} and m_{V_2}, then, after a transient, two terms survive in the asymptotic behavior of $c_0(t)$, which thus oscillates at the frequencies m_{V_1} and m_{V_2}. Hence the appearance of a ghost state, in addition to the physical V state, is responsible for a beating in the probability $|c_0(t)|^2$ at the frequency $|m_{V_2} - m_{V_1}|$. Conversely, if only the physical V state does exist, $|c_0(t)|^2$ settles down to a constant value and does not oscillate. As will be discussed in Sec. III, the presence or the absence of an oscillation in the evolution of $|c_0(t)|^2$ can be easily visualized in our photonic simulator of the QFT Lee model.

B. An exactly solvable case

Let us specialize the general analysis briefly reviewed in the previous subsection to an exactly solvable model, which can be rather simply implemented in a photonic system as discussed in the next section. Let us assume the following forms for the spectral coupling function $f(k)$ and the dispersion relation $\omega(k) = \Omega(k) + m_{N_0}$:

$$f(k) = \sqrt{\frac{2}{\pi}} \sin k, \quad \omega(k) = \omega_0 - 2\kappa_0 \cos k, \tag{15}$$

where the quantum number k varies in the range $0 < k \leqslant \pi$, κ_0 is a positive constant that determines the energy width $4\kappa_0$ of the N-θ scattered states, $\omega_0 = \mu + 2\kappa_0 + m_{N_0}$, and μ is the lower limit of the dispersion curve $\Omega(k)$ (it plays the analogous role of the boson mass μ of Refs. [2,3,10]). It should be noted that, for a real bare coupling g, this model has been studied in different physical contexts as well, such as in problems of Fano resonances and bound states in the continuum (see, for instance, Refs. [21–24] and references therein). A non-Hermitian extension of the model was recently investigated in Ref. [25], where attention was primarily devoted to the investigation of spectral singularities. However, such a non-Hermitian model was not $\mathcal{PT}$ invariant and the analysis was not related to the Lee model in the ghost regime. Using Eq. (15), the spectral function $G(\omega)$ and $\Delta(m_V)$ can be calculated in a closed form and read

$$G(\omega) = \begin{cases} \frac{1}{\pi\kappa_0}\sqrt{1 - \left(\frac{\omega-\omega_0}{2\kappa_0}\right)^2}, & |\omega - \omega_0| < 2\kappa_0 \\ 0, & \text{otherwise,} \end{cases} \tag{16}$$

$$\Delta(m_V) = \begin{cases} \frac{1}{2\kappa_0^2}\left[\sqrt{(m_V - \omega_0)^2 - 4\kappa_0^2} + m_V - \omega_0\right], & m_V - \omega_0 < -2\kappa_0 \\ \frac{1}{2\kappa_0^2}(m_V - \omega_0), & |m_V - \omega_0| < 2\kappa_0 \\ \frac{1}{2\kappa_0^2}\left[-\sqrt{(m_V - \omega_0)^2 - 4\kappa_0^2} + m_V - \omega_0\right], & m_V - \omega_0 > 2\kappa_0. \end{cases} \tag{17}$$

We will limit our analysis to the case $m_{V_0} < \mu + m_{N_0}$, which ensures the stability of the physical V-particle state. Using Eq. (17), the bound states of $\hat{H}$ below the continuum (i.e., corresponding to $m_V < \mu + m_{N_0}$) can be readily calculated from Eq. (4), according to the graphical construction shown in Fig. 1(a). The results in parameter space (m_{V_0}, g_0) are summarized in Fig. 1(b). In particular, three cases should be distinguished.

(i) For $(g_0/\kappa_0) < \sqrt{-2 + (\omega_0 - m_{V_0})/(2\kappa_0)}$ [domain I in Fig. 1(b), delimited by curve 1], there exists a simple and real-valued root $m_V = m_{V_1}$ to Eq. (4), with $Z > 0$ (i.e., corresponding to the physical V particle) given by

$$m_{V_1} = m_{N_0} + \mu - 2\kappa_0(\cosh\mu_1 - 1), \tag{18}$$

where μ_1 is defined by

$$\exp(\mu_1) = -\frac{m_{V_0} - \omega_0}{2\kappa_0} + \sqrt{\frac{(m_{V_0} - \omega_0)^2}{4\kappa_0^2} - 1 - \left(\frac{g_0}{\kappa_0}\right)^2} \tag{19}$$

[case I of Fig. 1(a)].

(ii) For $\sqrt{-2 + (\omega_0 - m_{V_0})/(2\kappa_0)} < (g_0/\kappa_0) < \sqrt{-1 + (\omega_0 - m_{V_0})^2/(2\kappa_0)^2}$ [domain II in Fig. 1(b), delimited by curves 1 and 2], there exist two real-valued roots $m_V = m_{V_1}$ and $m_V = m_{V_2} > m_{V_1}$ to Eq. (4), which are given by

$$m_{V_j} = m_{N_0} + \mu - 2\kappa_0(\cosh\mu_j - 1) \tag{20}$$

with $j = 1$ or 2 and where μ_1 and μ_2 are defined by

$$\exp(\mu_1) = -\frac{m_{V_0} - \omega_0}{2\kappa_0} + \sqrt{\frac{(m_{V_0} - \omega_0)^2}{4\kappa_0^2} - 1 - \left(\frac{g_0}{\kappa_0}\right)^2},$$
$$\exp(\mu_2) = -\frac{m_{V_0} - \omega_0}{2\kappa_0} - \sqrt{\frac{(m_{V_0} - \omega_0)^2}{4\kappa_0^2} - 1 - \left(\frac{g_0}{\kappa_0}\right)^2} \tag{21}$$

[case II of Fig. 1(a)]. For the former solution m_{V_1}, one has $Z > 0$, (i.e., it corresponds to the physical V-particle state); however, for the latter solution m_{V_2}, it turns out that $Z < 0$ (i.e., this additional solution corresponds to a ghost state).

(iii) For $(g_0/\kappa_0) > \sqrt{-1 + (\omega_0 - m_{V_0})^2/(2\kappa_0)^2}$ [domain III in Fig. 1(b), delimited by curve 2], there are two complex-conjugate roots to Eq. (4). In such a domain, the $\mathcal{PT}$ phase of $\hat{H}$ is broken. This case will not be considered further here.

It should be noted that, as the boundary between domains II and III is approached from domain II [curve 2 in Fig. 1(b), corresponding to $g_0^2 = 1/L$], the two states corresponding to m_{V_1} and m_{V_2} coalesce [see the dashed curve in Fig. 1(a)] and

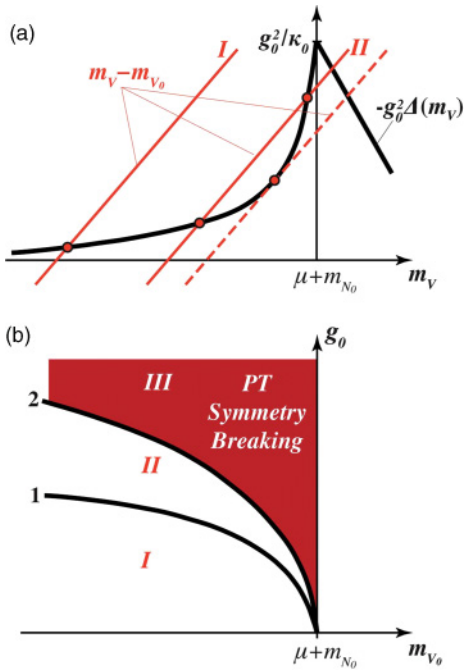

FIG. 1. (Color online) (a) Graphical construction for the determination of bound states of the $\mathcal{PT}$-symmetric Lee Hamiltonian with spectral coupling and dispersion relation defined by Eq. (15). The eigenvalues m_V of bound states are obtained as the intersection of the straight line $m_V - m_{V_0}$ with the curve $-g_0^2\Delta(m_V)$, where $\Delta(m_V)$ is given by Eq. (17). In case I there is only one intersection, corresponding to the physical V-particle state with a positive norm. In case II there are two intersections, one with a negative norm corresponding to a ghost state. The dashed straight line corresponds to the boundary of $\mathcal{PT}$ symmetry breaking, where the two intersections coalesce. (b) Domain of existence of bound states for the Lee Hamiltonian in the (m_{V_0}, g_0) plane. In domain I, there exists solely one bound state, corresponding to the physical V-particle state. In domain II there are two bound states, the additional one being a ghost state. In domain III a pair of complex-conjugate energies appears (broken $\mathcal{PT}$ phase). The analytical expression of curves 1 and 2, that define the boundaries of the three domains, are given in the text.

$Z \to \infty$ according to Eq. (11): hence at the $\mathcal{PT}$ symmetry-breaking boundary two complex-valued energies bifurcate from the coalescence of the two real-valued branches (20) and an exceptional point, signaled by the vanishing of $\langle\psi_1^*|\psi_2\rangle$, appears [see Eq. (10)].

III. OPTICAL REALIZATION OF $\mathcal{PT}$-SYMMETRIC LEE MODEL

An optical simulation of the $\mathcal{PT}$-symmetric Lee model, described in Sec. II B, can be realized by mapping the *temporal* evolution of the probability amplitudes $c_0(t)$ and $\Phi(k,t)$ of bare V-particle and N-θ scattering states, governed by Eqs. (13) and (14), into *spatial* propagation of light waves in suitably engineered arrays of evanescently coupled optical waveguides [26]. In fact, Eqs. (13) and (14) describe quite generally the decay dynamics of a bound state coupled to a continuum and, as shown in Refs. [24,27], this problem can be simulated in an optical setup based on light transport in a semi-infinite waveguide lattice. However, to simulate the Lee model in the ghost regime, we need to realize an *imaginary* coupling $g = ig_0$ between the bound state and the continuum of scattering states, and this possibility was not addressed in such previous works. As we will show here, an imaginary coupling g can be realized by considering either second-order nonlinear interactions in the boundary waveguide of the semi-array, or a suitable fast modulation of both the real and imaginary parts of the refractive index of the boundary waveguide.

To provide an optical simulation of Eqs. (13) and (14), following Ref. [24] let us notice that, since k varies in the range $0 < k < \pi$, we can expand $\Phi(k,t)$ as a Fourier series of sine terms solely according to

$$\Phi(k,t) = -\sqrt{\frac{2}{\pi}} \sum_{n=1}^{\infty} c_n(t) \sin(nk), \tag{22}$$

and the inversion relation

$$c_n(t) = -\sqrt{\frac{2}{\pi}} \int_0^{\pi} dk \Phi(k,t) \sin(nk) \tag{23}$$

$(n = 1,2,3,\ldots)$ holds. Taking into account that $\int_0^{\pi} dk \sin(nk)\sin(mk) = (\pi/2)\delta_{n,m}$, the evolution equations of the amplitudes c_n can be readily derived using Eqs. (13), (14), (22), and (23) and read

$$i\frac{dc_n}{dt} = -\kappa_0(c_{n+1} + c_{n-1}) + \omega_0 c_n \ (n \geqslant 2), \tag{24}$$

$$i\frac{dc_1}{dt} = -\kappa_0 c_2 - ig_0 c_0 + \omega_0 c_1, \tag{25}$$

$$i\frac{dc_0}{dt} = -ig_0 c_1 + m_{V_0} c_0. \tag{26}$$

In their present forms, Eqs. (24)–(26) describe light transport of monochromatic light waves in a semi-infinite array of optical waveguides [see Fig. 2(a)], in which κ_0 is the coupling constant and ω_0 in the propagation constant of the guided modes in the waveguides $n \geqslant 1$ (i.e., except for the boundary waveguide), m_{V_0} is the propagation constant of the boundary waveguide $n = 0$, ig_0 is the complex-valued coupling constant between the waveguides $n = 0$ and $n = 1$ in the lattice, and t is the longitudinal spatial coordinate of the array, as shown in Fig. 2(a). A major issue that should be addressed for a physical realization of the tight-binding lattice model Eqs. (24)–(26) is the request to implement an imaginary coupling rate: in fact, evanescent coupling of optical fields between two coupled dielectric optical waveguides generally leads to an effective real-valued coupling (after a suitable choice of the phase of the propagating field amplitudes). To realize an effective imaginary coupling, we must consider a non-Hermitian optical setup.

A first possibility, briefly sketched in Fig. 2(b), consists of considering a semi-array of waveguides manufactured in a nonlinear $\chi^{(2)}$ optical medium. The boundary waveguide of the semi-array is designed to sustain three modes of different frequencies ω_1 (the signal field), ω_2 (the idler field), and $\omega_3 = \omega_1 + \omega_2$ (the pump field) which are phase matched via a quasi-phase-matching (QPM) grating (see, for instance, Ref. [28]). For a strong pump field and weak signal and idler

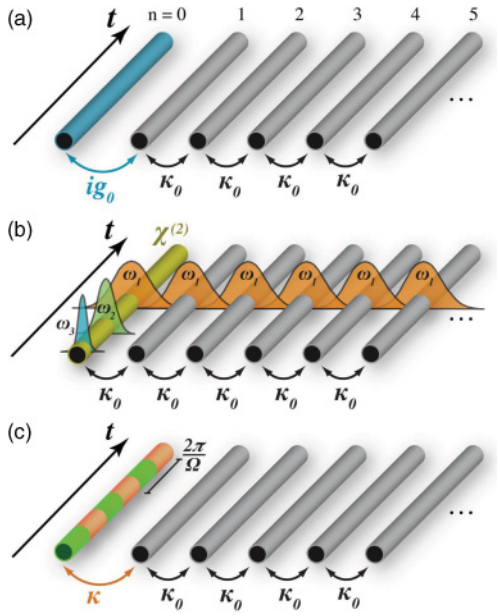

FIG. 2. (Color online) (a) Schematic of the optical realization of the $\mathcal{PT}$-symmetric Lee model discussed in Sec. II B, based on light transport in a semi-infinite array of evanescently coupled optical waveguides. In the optical analog, the longitudinal propagation distance t plays the role of time in the QFT model. The complex coupling $g = ig_0$ of the Lee Hamiltonian in the ghost regime requires a complex coupling between the boundary waveguides in the semi-array. Panels (b) and (c) show two possible optical implementations of such a complex coupling. In panel (b), a semi-infinite array of waveguides with a second-order $\chi^{(2)}$ nonlinearity is considered, in which parametric amplification between signal and idler fields at frequencies ω_1 and ω_2 is allowed in the boundary waveguide via a QPM grating. The signal field is then evanescently coupled to the other waveguides in the array, where propagation is linear. In panel (c) the complex coupling $g = ig_0$ is realized by introduction of a fast modulation of both real and imaginary parts of the effective refractive index in the boundary waveguide, with spatial period $2\pi/\Omega$. As discussed in the text, in the fast modulation limit and for appropriate modulation parameters, the waveguide lattice in (c) effectively behaves as the lattice in (a).

fields, in the no-pump-depletion limit the signal and idler modes in the boundary waveguide are coupled by an effective imaginary coupling ig_0, where g_0 is the parametric gain which is proportional to the intensity I_3 of the pump field and to the effective second-order susceptibility $d_{\rm eff}$ of the medium according to the relation $g_0 = 2\pi d_{\rm eff}\sqrt{2I_3/(n_1n_2n_3\lambda_1\lambda_2c_0\epsilon_0)}$, where n_k are the refractive indices of the signal, idler, and pump waves at wavelengths λ_k ($k = 1,2,3$) [28,29]. The other waveguides in the semi-array lack of the QPM grating, so that frequency conversion does not take place there and light propagates in the linear regime. The waveguides are designed such as the field at frequency ω_1 is close to a cutoff (i.e., it is weakly confined), whereas the modes at frequencies ω_2 and ω_3 are well confined. In this way, evanescent coupling between adjacent waveguides is mostly effective for the signal field at frequency ω_1, whereas it may be neglected for both the idler and pump fields. Therefore, in such a system, light propagation is described by Eqs. (24)–(26), where c_0 and c_1 correspond to the modal amplitudes of the fields at frequencies ω_2 and ω_1, respectively, propagating in the boundary waveguide, whereas the c_n ($n \geqslant 2$) correspond to the modal amplitudes of the field at frequency ω_1 trapped in the other waveguides of the semi-array. The complex coupling ig_0 is realized by the parametric gain in the boundary waveguide, which can be conveniently tuned by varying the intensity I_3 of the pump wave.

A second possibility consists of considering a semi-infinite waveguide array in which a longitudinal modulation of both optical gain or absorption and effective modal index in the boundary waveguide is introduced, as schematically shown in Fig. 1(c). In this case, in the tight-binding and nearest-neighboring approximations, the coupled-mode equations describing light propagation in the non-Hermitian waveguide lattice of Fig. 1(c) read

$$i\frac{dc_n}{dt} = -\kappa_0(c_{n+1} + c_{n-1}) + \omega_0 c_n \ (n \geqslant 2), \tag{27}$$

$$i\frac{dc_1}{dt} = -\kappa_0 c_2 - \kappa a_0 + \omega_0 c_1, \tag{28}$$

$$i\frac{da_0}{dt} = -\kappa c_1 + [m_{V_0} - A\cos(\Omega t)]a_0, \tag{29}$$

where κ is the real-valued coupling constant between waveguides $n = 0$ and $n = 1$, Ω is the spatial modulation frequency of the complex-valued modulated propagation constant in the guide $n = 0$, $A = A_R + iA_I$ is the modulation amplitude, c_n ($n \geqslant 1$) are the modal amplitudes of light trapped in waveguides with index $n \geqslant 1$, and a_0 is the modal amplitude of light trapped in the boundary waveguide $n = 0$. Physically, the real part of A accounts for the longitudinal sinusoidal modulation of the effective modal index, whereas the imaginary part of A describes the longitudinal modulation of the optical gain or absorption in the boundary waveguide. The t-independent lattice model of Eqs. (24)–(26) can be obtained as a first-order approximation from the t-periodic lattice model of Eqs. (27)–(29) in the large-modulation limit $\Omega \gg \kappa_0, \kappa, |\omega_0 - m_{V_0}|$, with A/Ω finite and of order ~ 1, by a multiple-scale asymptotic analysis (see, for instance, Ref. [30]). Let us introduce, in place of $a_0(t)$, the new variable $c_0(t) = a_0(t)\exp[-i\Gamma\sin(\Omega t)]$, where we have set $\Gamma = A/\Omega$. Then Eqs. (27)–(29) can be written in the equivalent form

$$i\frac{dc_n}{dt} = -\kappa_0(c_{n+1} + c_{n-1}) + \omega_0 c_n \ (n \geqslant 2), \tag{30}$$

$$i\frac{dc_1}{dt} = -\kappa_0 c_2 - \kappa\exp[i\Gamma\sin(\Omega t)]c_0 + \omega_0 c_1, \tag{31}$$

$$i\frac{dc_0}{dt} = -\kappa\exp[-i\Gamma\sin(\Omega t)]c_1 + m_{V_0}c_0. \tag{32}$$

An exact analysis of Eqs. (30)–(32) would require the determination of quasi-energies by Floquet theory; in particular, we are interested in exploring the parameter space where the quasi-energies remain real (in spite of the non-Hermiticity of the system); this would correspond to the unbroken $\mathcal{PT}$ phase of the Lee model. In the fast-modulation limit, at leading order in the analysis, the rapidly oscillating terms in Eqs. (31) and (32) can be replaced by their averaged values over one

oscillation cycle (see, for instance, [30]); that is, one can write

$$i\frac{dc_n}{dt} \simeq -\kappa_0(c_{n+1}+c_{n-1})+\omega_0 c_n \ (n \geqslant 2), \tag{33}$$

$$i\frac{dc_1}{dt} \simeq -\kappa_0 c_2 - \kappa_e c_0 + \omega_0 c_1, \tag{34}$$

$$i\frac{dc_0}{dt} \simeq -\kappa_e c_1 + m_{V_0} c_0, \tag{35}$$

where we have set

$$\kappa_e = \kappa J_0\left(\frac{A}{\Omega}\right), \tag{36}$$

where J_0 is the Bessel function of first kind of zero order. Hence, if the ratio between the *complex* modulation amplitude A and the modulation frequency Ω is chosen such that κ_e is purely imaginary, the effective lattice model described by Eqs. (33)–(35) reduces to that of Eqs. (24)–(26), with $ig_0 = \kappa_e$; that is, it realizes the $\mathcal{PT}$-symmetric QFT Lee model introduced in Sec. II B.

As discussed at the end of Sec. II A, the appearance of a ghost state in addition to the physical V-particle state can be monitored by the temporal evolution of $|c_0(t)|^2$, when the system is initially prepared in the bare V state. In the optical setting of Fig. 3(c), such an initial condition corresponds to the excitation, at the input $t = 0$ plane, of the boundary waveguide $n = 0$ [i.e., to $c_n(0) = \delta_{n,0}$ in Eqs. (30)–(32)], whereas in the optical setting of Fig. 3(b) this corresponds to initial excitation of the boundary waveguide by the idler field. In the parameter region corresponding to domain I of Fig. 1(b), there is only one bound state (the physical V state), and hence after an initial transient $|c_0(t)|^2$ sets to a constant and nonvanishing value. This is shown, as an example, in Fig. 3(a), which depicts the evolution of $|c_0(t)|^2$ for parameter values $g_0/\kappa_0 = 0.91$ and $(m_{V_0} - \omega_0)/\kappa_0 = -4$. In the figure, the behavior of $|c_0(t)|^2$, predicted by the Lee model [Eqs. (24)–(26), dotted curve in Fig. 3(a)], is compared with that obtained by numerical analysis of the time-periodic system [Eqs. (30)–(32), solid curve in Fig. 3(a)], corresponding to the optical realization of Fig. 3(c). As g_0 is increased to cross domain II, the appearance of the ghost state, in addition to the physical V state, changes the asymptotic behavior of $|c_0(t)|^2$, which is now oscillatory at the frequency $|m_{V_1} - m_{V_2}|$, as shown in Fig. 3(b). As the upper boundary of domain II is approached [i.e., if we move toward curve 2 in Fig. 1(b)], the period of the oscillation increases, as shown in Fig. 3(c). In the photonic realization of the modulated lattice of Fig. 2(c), we assumed a modulation frequency $\Omega/\kappa_0 = 15$ and a normalized complex modulation parameter $\Gamma = A/\Omega \simeq 2 - 1.996i$, leading to an imaginary value $\kappa_e = ig_0$, according to Eq. (36). The increase of g_0, from Figs. 3(a) to 3(c), is obtained, in the realization of Fig. 3(b), by simply increasing the parametric gain (i.e., by an increase of the pump intensity I_3), whereas in the optical realization of Fig. 3(c) an increase of g_0 can be achieved by simply increasing the coupling constant κ, i.e., by diminishing the distances of waveguides $n = 0$ and $n = 1$.

To get an estimate of the parameter values in physical units corresponding to the simulations shown in Fig. 3, let us consider for instance the optical implementation of Fig. 2(b), based on a nonlinear waveguide array, which seems to be the more accessible experimental system [31]. Let us consider a semi-array of periodically poled lithium-niobate (PPLN) waveguides, with pump, signal, and idler waves at wavelengths $\lambda_3 = 532$ nm, $\lambda_1 = 1.55$ μm, and $\lambda_2 = 810$ nm, respectively. For the PPLN crystal at 25 °C, a QPM grating of the nonlinear $\chi^{(2)}$ susceptibility with spatial period $\Lambda \simeq 7.39$ μm is required in the boundary waveguide to phase match the frequency conversion process (see, for instance, Ref. [29]). Let us assume a typical coupling constant of adjacent waveguides for the signal modes of $\kappa_0 = 2$ cm^{-1}. Correspondingly, the physical unit of propagation length in the horizontal axis of Fig. 3 is 0.5 cm, so that for a sample of length 10 cm the dynamics shown in Fig. 3 can be observed up to $\kappa_0 t = 20$. The levels of parametric gain g_0 required to observe the dynamics shown in Figs. 3(a)–3(c) are given by $g_0 \simeq 1.820$, 3.094, and 3.276 cm^{-1}, respectively, whereas the detuning between the propagation constant of the boundary waveguide, for the signal field, and the other waveguides in the array turns out to be $4\kappa_0 = 8$ cm^{-1}. Such a detuning can be readily achieved by a

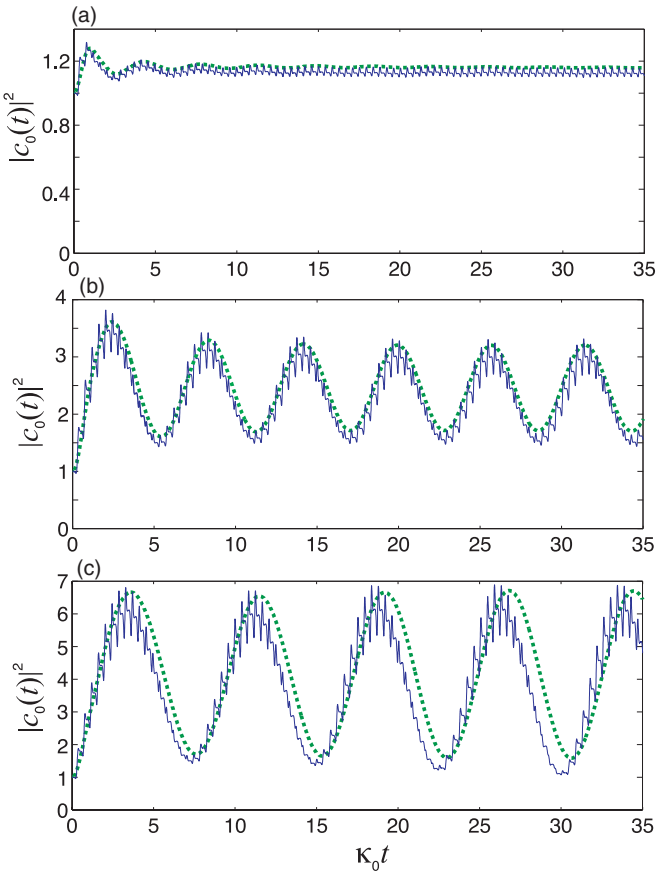

FIG. 3. (Color online) Behavior of $|c_0(t)|^2$; that is, evolution of the probability of the bare particle state $\hat{V}^\dagger|0\rangle$ versus normalized time $\kappa_0 t$ for the initial condition $c_0(0) = 0$, $\Phi(k,0) = 0$, detuning $m_{V_0} - \omega_0 = -4\kappa_0$, and for (a) $g_0/\kappa_0 = 0.91$, (b) $g_0/\kappa_0 = 1.547$, and (c) $g_0/\kappa_0 = 1.638$. The dotted curves are obtained by numerical analysis of Eqs. (24)–(26), which exactly reproduce the $\mathcal{PT}$-symmetric Lee model and are implemented by the optical system of Fig. 2(b). The solid curves in the figures refer to the numerical analysis of Eqs. (30)–(32), which describe the optical implementation of Fig. 2(c) based on fast modulation of the real and imaginary parts of the refractive index in the boundary waveguide.

suitable waveguide design. A parametric gain of the order of $g_0 \sim 3\ \mathrm{cm}^{-1}$ requires a pump level $I_3 \sim 22\ \mathrm{MW/cm}^2$ (taking $d_{\mathrm{eff}} \sim 17$ pm/V for first-order QPM in PPLN [29]); for an effective mode area $A_e \sim 6\ \mu\mathrm{m}^2$, this would correspond to a continuous-wave pump power of $P_3 \sim A_e I_3 \simeq 1.32$ W, which is a reasonable level for PPLN waveguides.

IV. CONCLUSIONS

In this work, we have proposed theoretically an optical realization of the QFT Lee model in the ghost regime, where the Lee Hamiltonian is non-Hermitian but $\mathcal{PT}$ symmetric [10] and ghost states appear. Our optical system is based on light transport in an engineered semi-infinite waveguide lattice, using either nonlinear parametric amplification in quadratic $\chi^{(2)}$ waveguides or suitable modulation of optical gain and absorption to mimic a complex coupling in the Lee model. It is envisaged that our results could stimulate further theoretical and experimental studies aimed to realize an accessible and feasible laboratory tool to simulate $\mathcal{PT}$-symmetric quantum field theories and to visualize the appearance and role of ghost states.

ACKNOWLEDGMENTS

This work was supported by the Italian MIUR (Grant No. PRIN-2008-YCAAK, "Analogie ottico-quantistiche in strutture fotoniche a guida d'onda"), and partially by the Fondazione Cariplo (Project "New Frontiers in Plasmonic Nanosensing", Rif. 2011-0338).

[1] K. W. Ford, Phys. Rev. **105**, 320 (1957).
[2] S. S. Schweber, *An Introduction to Relativistic Quantum Field Theory* (Row, Peterson, and Co., Evanston, 1961), Chap. 12.
[3] G. Barton, *Introduction to Advanced Field Theory* (John Wiley & Sons, New York, 1963), Chap. 12.
[4] T. D. Lee, Phys. Rev. **95**, 1329 (1954).
[5] G. Källen and W. Pauli, Mat. Fys. Medd. **30**(7) (1955).
[6] C. M. Bender and S. Boettcher, Phys. Rev. Lett. **80**, 5243 (1998); C. M. Bender, D. C. Brody, and Hugh F. Jones, *ibid.* **89**, 270401 (2002).
[7] C. M. Bender, Rep. Prog. Phys. **70**, 947 (2007).
[8] A. Mostafazadeh, Phys. Scr. **82**, 038110 (2010).
[9] C. M. Bender, K. A. Milton, and V. M. Savage, Phys. Rev. D **62**, 085001 (2000); C. M. Bender, D. C. Brody, and H. F. Jones, Phys. Rev. Lett. **93**, 251601 (2004); Phys. Rev. D **70**, 025001 (2004); C. M. Bender, S. F. Brandt, J.-H. Chen, and Q. Wang, *ibid.* **71**, 065010 (2005); C. M. Bender and P. D. Mannheim, Phys. Rev. Lett. **100**, 110402 (2008); A. M. Shalaby, Phys. Rev. D **80**, 025006 (2009); A. Mostafazadeh, *ibid.* **84**, 105018 (2011).
[10] C. M. Bender, S. F. Brandt, J.-H. Chen, and Q. Wang, Phys. Rev. D **71**, 025014 (2005).
[11] A. Ruschhaupt, F. Delgado, and J. G. Muga, J. Phys. A **38**, L171 (2005).
[12] R. El-Ganainy, K. G. Makris, D. N. Christodoulides, and Z. H. Musslimani, Opt. Lett. **32**, 2632 (2007); K. G. Makris, R. El-Ganainy, D. N. Christodoulides, and Z. H. Musslimani, Phys. Rev. Lett. **100**, 103904 (2008).
[13] S. Klaiman, U. Günther, and N. Moiseyev, Phys. Rev. Lett. **101**, 080402 (2008).
[14] A. Mostafazadeh, Phys. Rev. Lett. **102**, 220402 (2009).
[15] A. Guo, G. J. Salamo, D. Duchesne, R. Morandotti, M. Volatier-Ravat, V. Aimez, G. A. Siviloglou, and D. N. Christodoulides, Phys. Rev. Lett. **103**, 093902 (2009); C. E. Rüter, K. G. Makris, R. El-Ganainy, D. N. Christodoulides, M. Segev, and D. Kip, Nature Phys. **6**, 192 (2010); T. Kottos, *ibid.* **6**, 166 (2010).
[16] S. Longhi, Phys. Rev. Lett. **105**, 013903 (2010).
[17] S. Longhi, Phys. Rev. A **82**, 031801 (2010); H. Ramezani, T. Kottos, R. El-Ganainy, and D. N. Christodoulides, *ibid.* **82**, 043803 (2010); A. A. Sukhorukov, Z. Xu, and Y. S. Kivshar, *ibid.* **82**, 043818 (2010); H. Ramezani, T. Kottos, R. El-Ganainy, and D. N. Christodoulides, *ibid.* **82**, 043803 (2010); S. Longhi, *ibid.* **82**, 031801 (2010); M. C. Zheng, D. N. Christodoulides, R. Fleischmann, and T. Kottos, *ibid.* **82**, 010103 (2010); Y. D. Chong, Li Ge, and A. D. Stone, Phys. Rev. Lett. **106**, 093902 (2011); Li Ge, Y. D. Chong, S. Rotter, H. E. Türeci, and A. D. Stone, Phys. Rev. A **84**, 023820 (2011); Z. Lin, H. Ramezani, T. Eichelkraut, T. Kottos, H. Cao, and D. N. Christodoulides, Phys. Rev. Lett. **106**, 213901 (2011); S. V. Dmitriev, S. V. Suchkov, A. A. Sukhorukov, and Y. S. Kivshar, Phys. Rev. A **84**, 013833 (2011); A. E. Miroshnichenko, B. A. Malomed, and Y. S. Kivshar, *ibid.* **84**, 012123 (2011); S. Longhi, J. Phys. A **44**, 485302 (2011); A. Mostafazadeh, Phys. Rev. A **84**, 023809 (2011).
[18] A. Szameit, M. C. Rechtsman, O. Bahat-Treidel, and M. Segev, Phys. Rev. A **84**, 021806 (2011).
[19] L. Feng, M. Ayache, J. Huang, Y. L. Xu, M. H. Lu, Y. F. Chen, Y. Fainman, and A. Scherer, Science **333**, 729 (2011); H. Benisty *et al.*, Opt. Express **19**, 18004 (2011); F. Nazari, M. Nazari, and M. K. Moravvej-Farshi, Opt. Lett. **36**, 4368 (2011).
[20] J. Schindler, A. Li, M. C. Zheng, F. M. Ellis, and T. Kottos, Phys. Rev. A **84**, 040101 (2011).
[21] G. D. Mahan, *Many-Particle Physics* (Plenum Press, New York, 1990), pp. 272–285.
[22] M. Cini, *Topics and Methods in Condensed-Matter Theory* (Springer, Heidelberg, 2007), Chap. 5, pp. 81–89.
[23] S. Tanaka, S. Garmon, and T. Petrosky, Phys. Rev. B **73**, 115340 (2006); S. Tanaka, S. Garmon, G. Ordonez, and T. Petrosky, *ibid.* **76**, 153308 (2007); H. Nakamura, N. Hatano, S. Garmon, and T. Petrosky, Phys. Rev. Lett. **99**, 210404 (2007).
[24] S. Longhi, Eur. Phys. J. B **57**, 45 (2007).
[25] S. Longhi, Phys. Rev. B **80**, 165125 (2009).
[26] We will focus here on the optical realization of the Lee model discussed in Sec. II B; however, other kinds of energy dispersion and spectral coupling functions could be simulated as well [see, for instance, S. Longhi, Phys. Rev. A **78**, 013815 (2008)].
[27] S. Longhi, Phys. Rev. Lett. **97**, 110402 (2006); Opt. Lett. **32**, 557 (2007); P. Biagioni, G. Della Valle, M. Ornigotti,

M. Finazzi, L. Duo, P. Laporta, and S. Longhi, Opt. Express **16**, 3762 (2008); F. Dreisow, A. Szameit, M. Heinrich, T. Pertsch, S. Nolte, A. Tünnermann, and S. Longhi, Phys. Rev. Lett. **101**, 143602 (2008).

[28] T. Suhara and M. Fujimura, *Waveguide Nonlinear-Optic Devices* (Springer, Berlin, 2003), Chap. 10.

[29] S. Longhi, M. Marano, and P. Laporta, Phys. Rev. A **66**, 033803 (2002).

[30] S. Longhi, Phys. Rev. B **77**, 195326 (2008).

[31] The other optical implementation, shown in Fig. 2(c) and based on a fast modulation of the gain or absorption coefficient of the boundary waveguide, would require ultrastrong gain coefficients A_I (of the order of $\sim$50–200 cm^{-1}). As such large gains might, in principle, be realized using, for example, a semiconductor quantum-dot waveguide amplifier, its practical implementation seems to be less feasible than the optical realization of Fig. 2(b).